JNS

CLINICAL ARTICLE

Functional connectivity networks for preoperative brain mapping in neurosurgery

Michael G. Hart, MBChB,[1,2] Stephen J. Price, PhD,[2] and John Suckling, PhD[1]

[1]Brain Mapping Unit, Department of Psychiatry, and [2]Division of Neurosurgery, Department of Clinical Neurosciences, University of Cambridge, United Kingdom

OBJECTIVE Resection of focal brain lesions involves maximizing the resection while preserving brain function. Mapping brain function has entered a new era focusing on distributed connectivity networks at "rest," that is, in the absence of a specific task or stimulus, requiring minimal participant engagement. Central to this frame shift has been the development of methods for the rapid assessment of whole-brain connectivity with functional MRI (fMRI) involving blood oxygenation level–dependent imaging. The authors appraised the feasibility of fMRI-based mapping of a repertoire of functional connectivity networks in neurosurgical patients with focal lesions and the potential benefits of resting-state connectivity mapping for surgical planning.

METHODS Resting-state fMRI sequences with a 3-T scanner and multiecho echo-planar imaging coupled to independent component analysis were acquired preoperatively from 5 study participants who had a right temporoparietooccipital glioblastoma. Seed-based functional connectivity analysis was performed with InstaCorr. Network identification focused on 7 major functional connectivity networks described in the literature and a putative language network centered on Broca's area.

RESULTS All 8 functional connectivity networks were identified in each participant. Tumor-related topological changes to the default mode network were observed in all participants. In addition, each participant had at least 1 other abnormal network, and each network was abnormal in at least 1 participant. Individual patterns of network irregularities were identified with a qualitative approach and included local displacement due to mass effect, loss of a functional network component, and recruitment of new regions.

CONCLUSIONS Resting-state fMRI can reliably and rapidly detect common functional connectivity networks in patients with glioblastoma and also has sufficient sensitivity for identifying patterns of network alterations. Mapping of functional connectivity networks offers the possibility to expand investigations to less commonly explored neuropsychological processes, such as executive control, attention, and salience. Changes in these networks may allow insights into mechanisms underlying the functional consequences of tumor growth, surgical intervention, and patient rehabilitation.

http://thejns.org/doi/abs/10.3171/2016.6.JNS1662

KEY WORDS default mode network; functional connectivity; glioblastoma; InstaCorr; ME-ICA; multiecho independent component analysis; resting-state functional MRI; seed-based connectivity; oncology; diagnostic and operative techniques

Neurosurgical management of focal brain lesions is based on the tenet that a more accurate and extensive resection is often closely correlated with successful outcomes, but only if resection can be achieved while preserving (or even improving) brain function.[33,49,50] Function therefore constrains resection and ultimately the success of much of what is attempted in neurosurgery. Accordingly, understanding functional neuroanatomy is fundamental to the advancement of neurosurgery.

Functional brain mapping has a rich history involving many modalities[9,14,34] and has been aided by significant contributions from the neurosurgical community.[17] Perspectives on brain mapping were originally directed toward a localization approach—whereby distinct functions are subserved by activities in distinct brain regions—which has proven successful, particularly in identifying the functions of the primary cortices. A more recent construct has viewed the brain as a set of interlocking, distributed

ABBREVIATIONS BOLD = blood oxygenation level–dependent; DMN = default mode network; fMRI = functional MRI; ME-ICA = multiecho independent component analysis; MNI = Montreal Neurological Institute; rsfMRI = resting-state fMRI; SCA = seed-based connectivity analysis; SMN = sensorimotor network.

SUBMITTED January 8, 2016. **ACCEPTED** June 8, 2016.
INCLUDE WHEN CITING Published online August 26, 2016; DOI: 10.3171/2016.6.JNS1662.

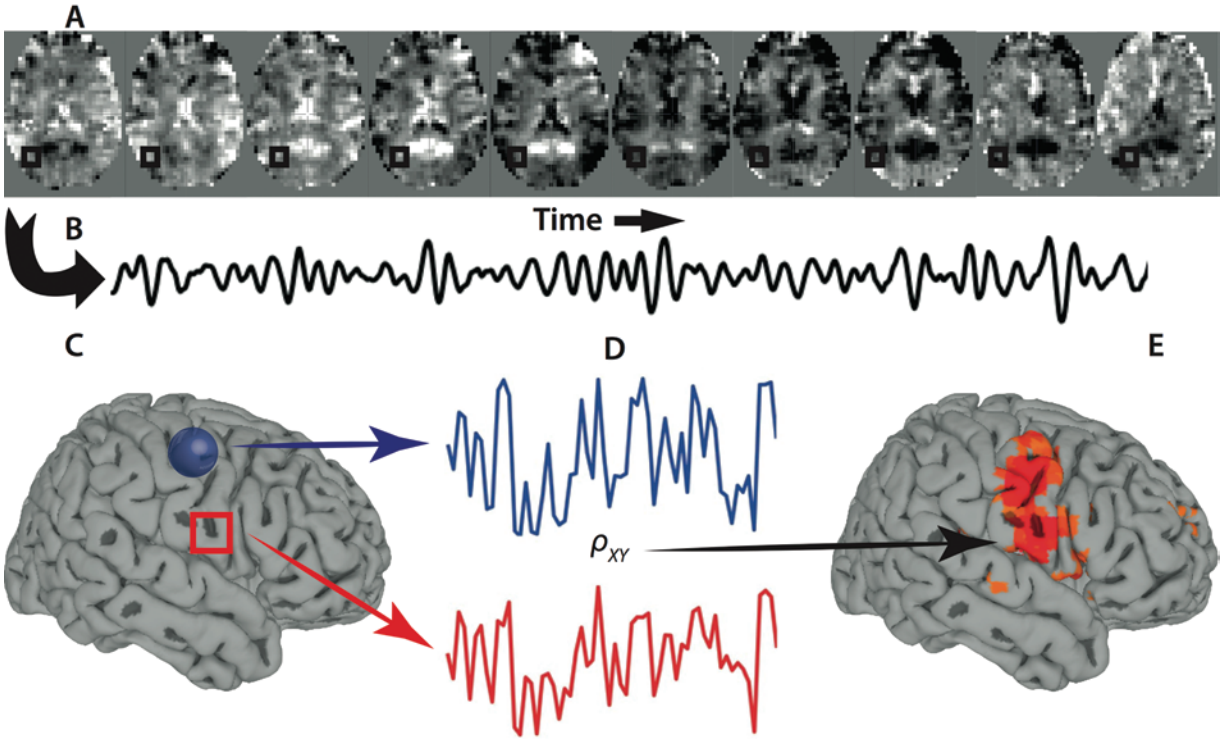

FIG. 1. The SCA method. **A:** An rsfMRI sequence (in the present study, a multiecho echo-planar imaging series) acquired 269 whole-brain 3D volumes over the scanning period (1 volume was acquired in 2.42 sec [the TR], yielding a total acquisition time of 10 min and 51 sec). The *black box* in the left lower brain region illustrates how the BOLD contrast changed over time. **B:** Each voxel therefore has a signal contrast change over time or the time series, which is shown here, with the time series of the region highlighted by the black box. **C:** A seed (in *blue*) is chosen depending on, for example, previous literature findings, a scientific hypothesis, or task-based activation. We selected a seed in the middle precentral gyrus and used a *red box* to highlight a region in the inferior precentral gyrus. The cortical reconstruction here was performed with the AFNI surface mapper SUMA (http://afni.nimh.nih.gov/afni/suma). **D:** The time series of this seed (in *blue*) is then compared with the time series of all other voxels, involving a measure of statistical correlation, most commonly Pearson correlation. Here, we used the area in the *red box* to show how the time series were compared. For SCA, however, all voxels were compared in a mass-univariate comparison independent of the seed time series. **E:** The voxel-wise correlation coefficients are rendered on the same cortical surface and thresholded to display those with a specified correlation (e.g., R > 0.5) Note, important preprocessing steps for both the rsfMRI scans and structural images need to be carried out before SCA. Figure is available in color online only.

processing networks. Synonymous with this approach has been the adoption of "resting-state" (that is, when there is no external stimulus or specific cognitive task) functional MRI (fMRI) based on blood oxygenation level–dependent (BOLD) imaging. A key result of resting-state fMRI (rsfMRI) has been the observation of networks that self-organize at rest,[12,15,51] supporting the idea that metabolic increases associated with task activity contribute only a few percent of the total energy consumption of the brain.[38] Over the past 2 decades, the network-based approach, spurred on by findings particularly from rsfMRI but also other modalities,[5,39,57] has gained precedence to the extent that the literature focusing on functional integration now exceeds that on functional localization.[16]

One of the potential uses of rsfMRI is the mapping of functional connectivity networks, also known as resting-state networks. One method for identifying these networks is seed-based connectivity analysis (SCA), which involves extracting a time series from a selected seed region and then measuring its correlation with all other voxels in the brain (Fig. 1). A summary of canonical functional connectivity networks commonly described in the literature is presented in Table 1 and Fig. 2.[39] Adoption of rsfMRI in the neurosurgical patient population is attractive for many reasons, including rapid whole-brain mapping rather than regional constraint by a single task or set of tasks; identification of higher-order networks and nonfocal processes in addition to primary cortices; compliance independence, facilitating use of rsfMRI in populations not able to adequately perform tasks (e.g., because of motor or language deficits); and applicability to populations not typically suited for task-based experiments, such as children and anesthetized participants.[42,57]

Resting-state fMRI studies with neurooncology patients have been previously performed and have usually focused on the accuracy of mapping primary cortices by comparison with results from studies using cortical stimulation to map these cortices (Table 2).[6,20,25,28,31,35–37,40,56] However, one of the main advantages of rsfMRI is the potential for mapping out higher-order functional connectivity networks that are less amenable to cortical stimulation. We also note that fMRI studies should not be expected to

TABLE 1. Summary of previously described resting-state networks

Network	Seed location	Region	Proposed Function
DMN	Precuneus	Precuneus/pst cingulate area & lat parietal & medial prefrontal regions	Task-negative network w/ complex & ambiguous function potentially related in internal reflection & self-reference
Visual	Calcarine sulcus	Medial striate & extrastriate regions	Vision (including dorsal & ventral streams)
SMN	Central sulcus	Bilat central sulcus & adjacent gyri	Penfield homunculus; fine motor & cortical sensory function
Auditory	Heschl's gyrus	Bilat Heschl's gyrus	Cortical auditory function
Executive	Medial prefrontal regions	Frontal eye field, intraparietal sulcus, & middle temporal area	Typical task-positive network involved in working memory & focused attention
Salience	Ant cingulate cortex	Ant cingulate & bilat insular cortices	Integration of processed sensory data w/ internal cues to guide behavior
Attention (dorsal)	Pst, lat, & parietal regions	Lat prefrontal & dorsal parietal regions	Visuospatial control
Language	Broca's region	Broca-Wernicke-Geschwind circuit	Expressive, receptive, & repetitive language

Ant = anterior; pst = posterior.

agree perfectly with studies involving cortical stimulation, as these approaches map the brain with different biological processes (blood oxygenation status rather than neural activity), different physical signals (nuclear magnetic resonance rather than electrical impedance), and distinct experimental designs (naturalistic observations rather than direct experimental manipulation). Therefore, mapping of functional connectivity networks should be considered complementary to, rather than a replacement for, more traditional methods of brain activity mapping.

Given the potential academic and clinical advantages of rsfMRI, we set out to test if it could be applied to neurosurgical patients in a more extended fashion than has been explored previously. Specifically, we sought to use SCA to 1) explore whether the functional connectivity networks most commonly identified in healthy populations could also be identified in a cohort with intrinsic brain tumors, 2) assess whether functional connectivity networks could be used in a preoperative brain mapping scenario requiring rapid and robust acquisition with a minimum of user intervention, and 3) identify patterns of networks perturbed by the tumor to assess if the technique has the requisite sensitivity for detecting putative plasticity or recovery-related changes.

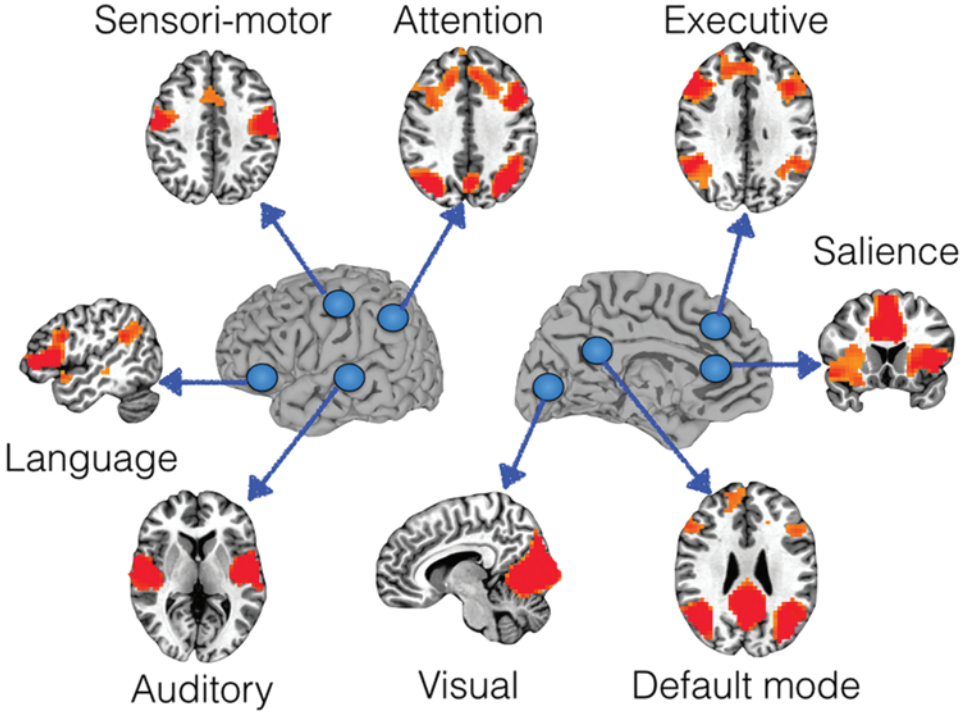

FIG. 2. Functional connectivity and resting-state networks. The 7 most commonly described canonical functional connectivity networks are displayed along with the corresponding seed locations that are used to build the networks (see Fig. 1). Also included was a putative language network derived from a seed in the left inferior frontal gyrus (Broca's region) because of the significance of this network for neurosurgical planning. Figure is available in color online only.

TABLE 2. Summary of rsfMRI studies in neurooncology patients

Authors & Year	No. of Pts	Pathology	Tumor Location	rsfMRI Analysis Method	Network of Interest	Comments
Sair et al., 2016	49	Gliomas w/ WHO Grades II (20 pts), III (12 pts), & IV (10 pts), & other (7 pts)	Lt hemisphere (38 pts); not otherwise specified	ICA w/ manually selected best match	Language	Variability in individual correspondence w/ task-based fMRI
Rosazza et al., 2014	13	Meningioma (1 pt), metastasis (2 pts), benign (3 pts), HGG (4 pts), LGG (2 pts), & lymphoma (1 pt)	Sensorimotor region & rt premotor region (8 pts)	ICA (best-match selection) & SCA (anatomical & task-based seeds)	SMN	Comparison w/ task-based fMRI & CS
Mitchell et al., 2013	7	Gliomas w/ WHO Grades II (5 pts) & IV (1 pt) & no surgery (1 pt)	Frontal (2 pts), frontoparietal (2 pts), frontotemporal (1 pt), parietal (1 pt), & temporal (1 pt)	MLP algorithm (artificial neural network)	Visual, dorsal & ventral attention, frontoparietal, DMN, SMN, & language	Agreement w/ CS; distorted SMN in 3 of 7 pts
Harris et al., 2014	68	Gliomas w/ WHO Grades II (21 pts), III (14 pts), & IV (33 pts)	Not specified	DMN template–based SCA	DMN	Pseudo-rsfMRI
Manglore et al., 2013	6	Brain tumor	Motor cortex (6 pts)	SCA	SMN	Comparison w/ task-based fMRI; reduced connectivity ipsilat to tumor
Böttger et al., 2011	8	Gliomas w/ WHO Grades I–IV & metastasis	Frontal (4 pts), central (3 pts), & parietal (1 pt) regions	Seed correlation (w/ Lipsia software)	SMN, language, DMN, & dorsal attention	Assessed clinical usability of a seed-based network tool
Zhang et al., 2009	4	HGG (3 pts) & metastasis (1 pt)	Frontoparietal region (4 pts)	SCA (4 pts) & SCA/ICA (1 pt) based on anatomical coordinates	SMN	Correlation w/ task-based fMRI & CS-assessed; SMN only
Liu et al., 2009	6	Gliomas w/ WHO Grade I–II (3 pts) & nontumor (3 pts)	Central (5 pts) & occipital (1 pt) regions; rt (3 pts), lt (2 pts), & bilat (1 pt) areas	SCA & manually identified anatomical seeds	SMN	Comparison w/ task-based fMRI; SMN only
Kokkonen et al., 2009	8	Meningioma (3 pts), cavernoma (2 pts), glioma w/ WHO Grades I (2 pts) & 3 (1 pt)	Frontal, temporal, parietal, & occipital tumors & their combinations (side not stated)	ICA & spatial cross-correlation template matching	SMN	Comparison w/ task-based fMRI; SMN only
Quigley et al., 2001	12	Tumor, cyst, AVM, & agenesis of corpus callosum	Nos. of each pathology, location, or hemisphere not specified	SCA w/ task fMRI seed locations	SMN & auditory, language	Network comparison w/ task-based fMRI activation maps

AVM = arteriovenous malformation; CS = cortical stimulation; HGG = high-grade glioma; ICA = independent component analysis; LGG = low-grade glioma; MLP = multilayer perceptron; pt(s) = patient(s).

Methods

Participants

The study was approved by the local regional ethics committee, and all participants provided written informed consent. Inclusion criteria were the appearance on MRI scans of a tumor consistent with glioblastoma, specifically inviting participation of patients with tumors in the right temporoparietooccipital region to gain a good approximation to a homogeneous sample. We chose this region for the following reasons. First, we wanted to include a homogeneous population. Second, we sought a location away from the main primary cortices that one would expect to find (e.g., language or motor areas). Last, there is emerging evidence that the nondominant parietal lobe has an important role in quality of life after glioma surgery, which suggests that a higher-order model of brain function (e.g., in resting-state networks) is required to better understand this phenomenon.

We included a cohort of 5 participants who were treated at our institution between April and June 2014 in the analysis. The basic demographic details of the study participants are summarized in Table 3. In brief, all of the participants had a glioblastoma confirmed by local histological review according to WHO criteria,[29] and all but 1 had complete resection of the contrast-enhancing tumor component as confirmed on a postoperative contrast-enhanced MRI scans within 72 hours of surgery.[54] Tumor locations in the 5 patients are shown in Fig. 3, indicating an overlap in tumor location and a homogeneous size among the patients.

TABLE 3. Demographics of the glioblastoma patients in this study

Case No.	Age (yrs)	Preop Exam Result	Op Extent	Tumor Location	Tumor Vol (cm^3)
1	64	Lt pronator drift	Complete resection	Rt superior parietal lobule	35.74
2	73	Intact	Complete resection	Rt inferior parietal lobule to occipital pole	86.30
3	79	Hemianopia	Complete resection	Rt inferior occipital lobe	46.23
4	76	Lt hemiparesis	Biopsy	Rt superior paracentral lobule	59.30
5	36	Lt hemiparesis	Complete resection	Rt postcentral gyrus & supramarginal gyrus	51.54

Imaging Parameters

The MRI data were acquired with a Siemens Trio 3-T scanner and 16-channel receive-only head coil (Siemens Medical Solutions). A multiecho echo-planar imaging sequence was acquired for 10 min and 51 sec at a TR of 2.42 sec per 3D volume, resulting in 269 3D volumes covering the cerebral cortices and cerebellum. Acquisition parameters were the following: flip angle 90°; matrix size 64 × 64; in-plane resolution 3.75 mm; TE 13.00 msec, 30.55 msec, and 48.10 msec; and slice thickness 3.8 mm. Anatomical images were acquired with a T1-weighted magnetization-prepared rapid gradient echo sequence (FOV 256 mm × 240 mm × 176 mm, matrix size 256 × 240 × 176, voxel size 1 mm isotropic, TR 2300 msec, TE 2.98 msec, and flip angle 9°).

fMRI Preprocessing

Data preprocessing was performed with AFNI[10] (http://afni.nimh.nih.gov/afni/) involving custom multiecho independent component analysis (ME-ICA) scripts.[26,27] The first 15 seconds of imaging data were discarded to allow for magnetization to reach a steady state. Subsequent steps included slice time correction, rigid-body motion correction, and de-spiking and de-obliquing. No spatial smoothing or bandpass filtering was performed at this stage.

Multiecho independent component analysis is a method for fMRI analysis and de-noising in a data-driven and physically principled manner and is based on the T2* decay of BOLD signals. As TE is varied, physiologically relevant BOLD contrast is expected to vary while noise remains stable. The behaviors of these 2 signals can be modeled with a pseudo-F statistic, resulting in 2 curves with distinct changes in gradient with BOLD contrast (κ) and noise (ρ). Multiecho fMRI time series are first decomposed into independent components with FastICA,[21] and each independent component is then categorized as either BOLD signal (high κ:ρ ratio) or noise (low κ:ρ ratio).

Magnetization-prepared rapid gradient echo structural scans were preprocessed with intensity normalization and brain extraction. Standard algorithms for brain extraction resulted in either significant residual nonbrain tissue or removal of intraaxial tissue. Therefore, we used the brain atlas of the Montreal Neurological Institute (MNI) defined in a stereotactic coordinate system transformed back into the acquisition spaces of each individual scan to mask the parenchyma of the brain, in a manner similar to that previously reported.[30] However, we used linear instead of nonlinear registration and hand-drawn masks of the contrast-enhancing tumor volume, and these masked areas were excluded from the registration cost function.

Last, all images were registered together to the MNI atlas at 2-mm resolution with the FSL package (http://fsl.fmrib.ox.ac.uk/fsl/fslwiki/) and FMRIB's Linear Image Registration Tool.[23,24] Registration parameters were optimized by selecting nearest-neighbor interpolation and using tumor masks as described above.

Seed-Based Connectivity Analysis

Correlation maps were created with the AFNI package InstaCorr.[11] The parameters set included automatic cortical masking, band pass filtering of 0.01–0.1 Hz, smoothing to 6-mm full width at half maximum, and seed defined as spheres of 10 mm diameter. The selection of seed locations was based on the literature on the most common and well-characterized resting-state networks (Table 1 and Fig. 2).[39,57] In addition, a putative language network was also sought with a seed in Broca's area in the left inferior frontal gyrus. Once a seed was selected, Pearson correlations between the mean time series of the seed-region voxels and all other voxels were calculated (Fig. 1). For consistency, we thresholded the correlation maps at R = 0.6 for all participants and networks.

We initially used the seed locations shown in Fig. 2, with a sphere having a radius of 10 mm. When a seed could be in either hemisphere (e.g., a central sulcus seed for the sensorimotor network [SMN]), we placed our seed in the left hemisphere (contralateral to the tumor). However, basing seed locations on coordinates may not be optimal

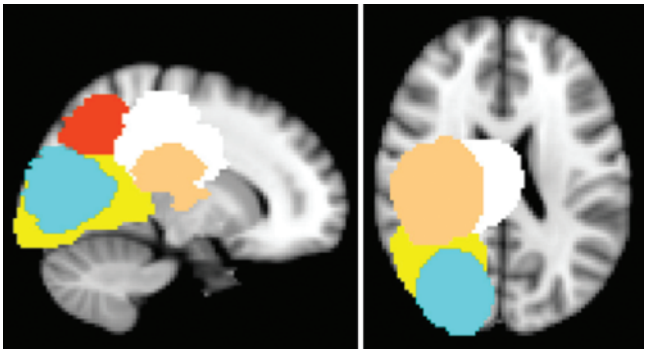

FIG. 3. Tumor locations in the 5 study participants. For each participant, a native-space tumor mask was hand drawn in FSLView and subsequently smoothed and registered to the MNI space in the sagittal (**left**) and axial (**right**) planes. Note the significant overlap in location and homogeneity in size among the patients. Figure is available in color online only.

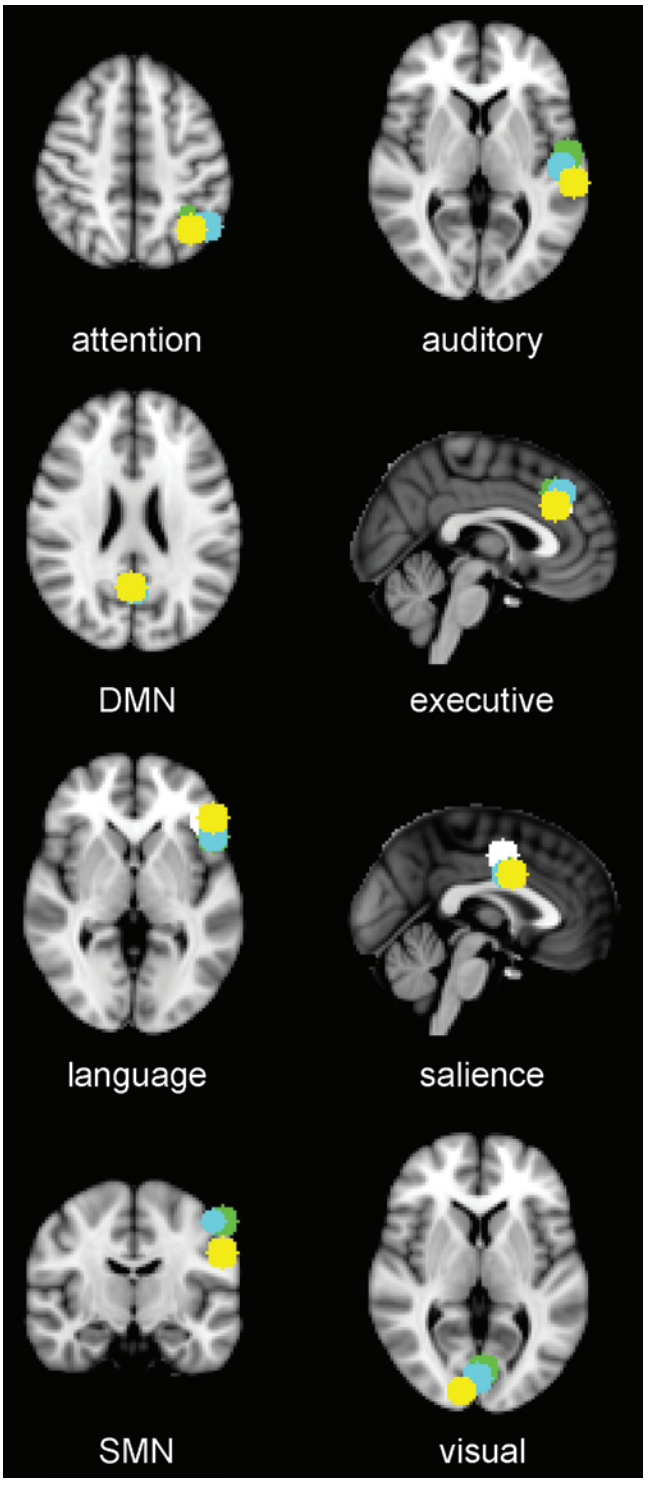

FIG. 4. Locations of the seeds used in functional connectivity analyses. The seed locations for each network were taken from Talairach coordinates in AFNI and were translated into 10-mm sphere masks in MNI space (1 sphere for each network per participant, i.e., 80 spheres in total). Each color represents a different seed for an individual participant. Only 2–3 different seed locations were required for each network, as the same seed coordinates could be used for some participants. Figure is available in color online only.

given individual differences in anatomy, standard-space registration, and functional connectivity.[32] One of the key advances of InstaCorr is that it allows flexible movement of the seed location while displaying the corresponding network in real time. Although the network produced is sensitive to seed location,[32] we constrained this flexibility by allowing our seeds to vary only within 10 mm of each other (corresponding to the radius of our seed) to create comparable networks across the participants with seeds that overlapped each other. Our aim was to balance homogeneous seed location with individual flexibility in seed location (Fig. 4).

Results

Individual Networks

The functional connectivity networks identified in the participants are summarized in Fig. 5. In each participant, we could identify the 7 canonical networks described in the literature, as well as a putative language network. The seed locations required to derive these networks exhibited a high degree of conformity, with the same location often used in several participants (Fig. 4). However, fine-tuning of the seed location was beneficial in selected instances to establish a network configuration resembling that described in the literature. In general, the auditory and attention networks were the most difficult to identify.

Summary Networks

The qualitative assessments of each functional connectivity network in each participant are summarized in Table 4. All participants had at least 2 networks that showed an alteration, and each network was altered in at least 1 participant, except for the language network, which was normal in all participants. The default mode network (DMN) was altered in all patients. The next most commonly altered network was the executive control network, which was altered in 4 patients.

Tumor location was closely related to determining which networks were affected. For example, tumors involving the superior parietal lobule (in Participants 1 and 2) affected the DMN and executive control network; tumors involving the occipital lobes (in Participants 2 and 3) affected the visual and DMN; and tumors that involved the anterior parietal region (in Participants 4 and 5) affected the SMN, DMN, and executive control network (Fig. 5).

Dynamic Alterations

One advantage of our cohort having tumors in approximately the same area was that we could look for patterns of alterations in our identified functional connectivity networks. Our whole-brain functional connectivity analysis suggested that in this cohort of participants with right temporoparietooccipital tumors, the DMN was most commonly altered from its normal topology (Fig. 5). Patterns appeared to represent local displacement (i.e., in Participant 4), novel topological area recruitment in combination with a reduction in the typical network architecture (in Participants 2 and 3), or an absence of a region typically associated with the network (in Participants 1 and 5). Interestingly, more posteriorly located tumors appeared to

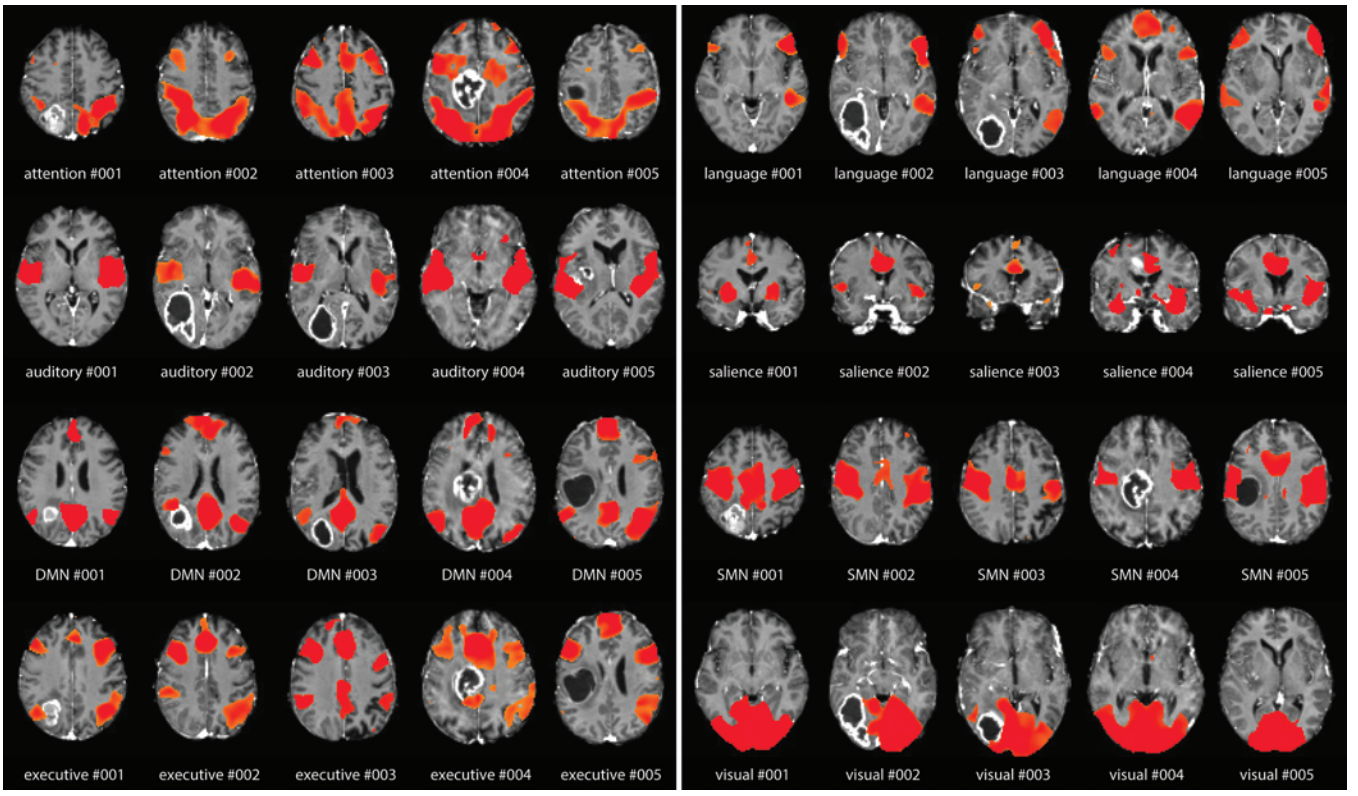

FIG. 5. Resting-state networks in each study participant. A single network is represented per row in each of the 2 panels, and each column represents a patient's representation of the networks (e.g., Column 3 is always Participant Number 3; numerals 001, 002, etc., represent Participant 1, Participant 2, etc., respectively). Putative plastic changes can be readily observed in the DMN but also in some other networks. In Participants 1 and 5, a notable reduction in the DMN is present in 1 hemisphere. In Participants 2 and 3, there is a reduction in DMN in the lateral parietal component with a new frontal area of activation. In Participant 4, the medial component of the DMN appears to be physically displaced rather than reduced in area, given that it is the same general size but mainly moved forward and is located immediately adjacent to the tumor. Figure is available in color online only.

result in new network areas, whereas the more anteriorly located tumors reduced network volume, but further data will be required to quantify these changes.

Discussion

Here, we have identified the most commonly described resting-state networks in a clinical cohort of study participants with glioblastoma. In addition, we were able to implement a refined preprocessing pipeline to resolve important fMRI challenges specific to neurooncology patients, including brain extraction, registration to normal space, de-noising, and seed-selection variability. Last, we identified tentative and qualitative patterns of network plasticity, particularly involving the DMN.

Previous neurosurgical studies involving rsfMRI have typically focused on the SMN, used a variety of techniques often yielding results that robustly correlate with the SMN mapped with cortical stimulation, and set in place early methodological achievements.[6,20,25,28,31,35–37,40,56] A key advancement of the present study was the identification of the full complement of functional connectivity networks. This advance was possible because of robust improvements in signal to noise achievable with ME-ICA preprocessing and the flexibility of seed selection available with InstaCorr. Having the full complement of functional connectivity networks available for preoperative planning is a significant step toward facilitating individually tailored surgery that maximizes resection while minimizing functional deficits.

Inference of the function associated with individual functional connectivity networks is based on their topologically distinct nature (i.e., the SMN is adjacent to the central sulcus, and the auditory network is centered on Heschl's gyrus). However, for those networks not centered on primary cortices, the cognitive and functional relevance may be less clear (Table 1). Moreover, when in the presence of a focal brain lesion a network is not found in its normal configuration, the question of whether this abnormality is a dynamic plastic change or indicates genuine functional impairment is more complex. Defining what a functional connectivity network is and what its dynamic alterations represent will require longitudinal imaging (pre- and post-surgery or during follow-up), correlation with neuropsychological outcomes, and use of multimodality monitoring (such as cortical stimulation, electroencephalography, magnetoencephalography, or other imaging modalities).

To develop our qualitative description of network changes into formal quantitative testing, robust statistical methods are needed, along with suitable control networks

TABLE 4. Summary of seed-connectivity networks identified in the 5 patients

Variable	Case No.				
	1	2	3	4	5
Tumor location	Parietal	Parietooccipital	Occipital	Frontoparietal	Temporoparietal
Network					
Attention	‡	†	*	*	*
Auditory	*	*	*	*	‡
DMN	‡	§	§	†	‡
Executive	†	†	*	†/‡	†
Language	*	*	*	*	*
Salience	*	*	*	‡	*
SMN	*	*	*	‡	‡
Visual	*	‡	§	*	*

* Network was normal.
† Network was reduced in area.
‡ Network locally shifted because of mass effect.
§ Network had reduced connectivity with new topological area, that is, network was asymmetrical.

for comparison. Although large databases of activities in neural pathways in healthy participants are now freely available (e.g., at www.humanconnectome.org),[43] statistical testing may be more complicated. Valid inference of seed-connectivity networks is not normally expected because of difficulties with calculating degrees of freedom; therefore, most studies use an arbitrary threshold for R of approximately 0.5.[26] With our ME-ICA technique, multiecho independent component regression can ensure valid inference. This technique takes the number of de-noised independent components as the degrees of freedom in the data and allows thresholding at a nominal p value (e.g., $p < 0.05$) based on z-scores or on more stringent comparisons involving a false-discovery rate. Studies in healthy controls have demonstrated robust connectivity networks with this method,[26] but we were unable to replicate these findings because of the de-noising process resulting in fewer surviving components and less representative networks. Nevertheless, we were able to use a correlation threshold of $R = 0.6$, which is larger than that usually applied.[26,27] A larger sample including participants with homogeneous disease would allow group analysis and effective multiecho independent component regression.

Once network function can be inferred, one needs also to understand what any alterations in a network's topology mean. For example, 1 scenario involves a network perturbation that might be expected to normalize with removal of a lesion and active rehabilitation of the patient, in turn correlating with clear neuropsychological improvement. However, robust testing of network changes may be challenging with seed-based connectivity methods because of the aforementioned issues. Ultimately, the role of SCA may be to rapidly estimate qualitative networks at the single-subject level for clinical practice, with the aim of observing perturbed or displaced networks that one may wish to avoid at surgery (see discussion below). Complex analyses aiming to model plasticity or predict cognitive changes from expanded extralesional resections may require sophisticated methods more suited to a research setting.[3,4,44,46]

The rapidity and ease of use of the method presented here suggest it could be adopted in clinical practice, perhaps even with surface renditions integrated into neuronavigation software. This would also have the advantage of including a wider range of tumor histologies and locations that will be necessary to validate the applicability of our new fMRI analysis method to the more diverse range of scenarios encountered in clinical practice. However, the aforementioned development required for improving our understanding of the neurocognitive basis of functional connectivity networks and the necessary improvements to statistical methods all suggest that a cautious approach should be adopted. For example, if the method reveals a functional connectivity network to be in close proximity to a tumor or the planned resection extent, counseling of the patient about the potential functional risks and goals of surgery could be warranted, possibly incorporating further monitoring (including awake craniotomy and cortical stimulation or other neurophysiological methods). In units that use cortical stimulation more routinely[13,41] or when extended resections are performed,[22] the functional connectivity networks identified could be used to guide the selection of tasks chosen for intraoperative testing to increase the specificity and efficiency of the assessments at surgery. The key message is that functional connectivity network analysis should be an additive component to preoperative surgical planning.

Seed-based functional connectivity methods are part of a larger repertoire of techniques available with rsfMRI. A similar method is independent component analysis, which also constructs distinct topological networks (some—but not all—of which are similar to those found in SCA). However, in a data-driven manner, independent component analysis is advantageous, as it offers higher dimensionality and robust statistical testing, but at the cost of being potentially more complex to perform; in addition, independent component analysis also results in networks that can be harder to relate to cognitive function.[3,4,44,45] Another avenue afforded by rsfMRI is complex network analysis by graph theory,[8,47,48] which may also be performed with other methods, including PET, electroencephalogra-

phy, magnetoencephalography, and diffusion imaging.[18,19] Graph theory analysis creates an abstract representation of the brain akin to that of a social network. The analysis then focuses on the properties of the graphical representation, its global or local efficiency, linkage of highly connected regions (known as a "hubs") to the overall network architecture, and so on.[52,53] A significant advantage of graph theory is its potential to model lesions and their effects on general network function.[1,2] Last, rsfMRI also enables the study of fractal dynamics, measured for example with the Hurst exponent,[55] which is a marker of brain complexity and potential for information processing.[7] In summary, rsfMRI, along with the various analysis methods to which it is allied, has the opportunity to address questions about functional brain mapping within neurosurgery.

Conclusions

We have found that rsfMRI offers an efficient method for whole-brain mapping of multiple functional connectivity networks in neurooncology patients before surgery. Method advancements to the processing pipeline make rsfMRI feasible for use in clinical practice and for further research, particularly in longitudinal studies invoking multimodality imaging and neuropsychological assessments. Further investigations of these techniques may reveal their potential for helping to predict cognitive deficits, increasing the extent of resection in a safe manner, and optimizing rehabilitation strategies according to the network derangements identified.

Acknowledgments

Dr. Price received funding for this study through a National Institute for Health Research (NIHR) (UK) - Clinician Scientist Award (ref: NIHR/CS/009/011). Mr. Hart is funded by the Wellcome Trust Neuroscience in Psychiatry Network with additional support from the National Institute for Health Research Cambridge Biomedical Research Centre.

References

1. Achard S, Salvador R, Whitcher B, Suckling J, Bullmore E: A resilient, low-frequency, small-world human brain functional network with highly connected association cortical hubs. **J Neurosci 26:**63–72, 2006
2. Alstott J, Breakspear M, Hagmann P, Cammoun L, Sporns O: Modeling the impact of lesions in the human brain. **PLOS Comput Biol 5:**e1000408, 2009
3. Beckmann CF, DeLuca M, Devlin JT, Smith SM: Investigations into resting-state connectivity using independent component analysis. **Philos Trans R Soc Lond B Biol Sci 360:**1001–1013, 2005
4. Beckmann CF, Smith SM: Probabilistic independent component analysis for functional magnetic resonance imaging. **IEEE Trans Med Imaging 23:**137–152, 2004
5. Biswal B, Yetkin FZ, Haughton VM, Hyde JS: Functional connectivity in the motor cortex of resting human brain using echo-planar MRI. **Magn Reson Med 34:**537–541, 1995
6. Böttger J, Margulies DS, Horn P, Thomale UW, Podlipsky I, Shapira-Lichter I, et al: A software tool for interactive exploration of intrinsic functional connectivity opens new perspectives for brain surgery. **Acta Neurochir (Wien) 153:**1561–1572, 2011
7. Bullmore E, Barnes A, Bassett DS, Fornito A, Kitzbichler M, Meunier D, et al: Generic aspects of complexity in brain imaging data and other biological systems. **Neuroimage 47:**1125–1134, 2009
8. Bullmore E, Sporns O: Complex brain networks: graph theoretical analysis of structural and functional systems. **Nat Rev Neurosci 10:**186–198, 2009
9. Catani M, ffytche DH: The rises and falls of disconnection syndromes. **Brain 128:**2224–2239, 2005
10. Cox RW: AFNI: software for analysis and visualization of functional magnetic resonance neuroimages. **Comput Biomed Res 29:**162–173, 1996
11. Cox RW: AFNI: what a long strange trip it's been. **Neuroimage 62:**743–747, 2012
12. Damoiseaux JS, Greicius MD: Greater than the sum of its parts: a review of studies combining structural connectivity and resting-state functional connectivity. **Brain Struct Funct 213:**525–533, 2009
13. Duffau H, Capelle L, Denvil D, Sichez N, Gatignol P, Taillandier L, et al: Usefulness of intraoperative electrical subcortical mapping during surgery for low-grade gliomas located within eloquent brain regions: functional results in a consecutive series of 103 patients. **J Neurosurg 98:**764–778, 2003
14. Finger S: **Origins of Neuroscience: A History of Explorations Into Brain Function.** Oxford: Oxford University Press, 2001
15. Fox MD, Raichle ME: Spontaneous fluctuations in brain activity observed with functional magnetic resonance imaging. **Nat Rev Neurosci 8:**700–711, 2007
16. Friston KJ: Functional and effective connectivity: a review. **Brain Connect 1:**13–36, 2011
17. Greenblatt S: Cerebral localization: from theory to practice. Paul Broca and Hughlings Jackson to David Ferrier and William Macewen, in Greenblatt SH, Dagi TF, Epstein MH (eds): **A History of Neurosurgery in its Scientific and Professional Contexts, ed 1.** Park Ridge, IL: American Association of Neurological Surgeons, 1997, pp 137–152
18. Hagmann P, Cammoun L, Gigandet X, Meuli R, Honey CJ, Wedeen VJ, et al: Mapping the structural core of human cerebral cortex. **PLoS Biol 6:**e159, 2008
19. Hagmann P, Kurant M, Gigandet X, Thiran P, Wedeen VJ, Meuli R, et al: Mapping human whole-brain structural networks with diffusion MRI. **PLoS One 2:**e597, 2007
20. Harris RJ, Bookheimer SY, Cloughesy TF, Kim HJ, Pope WB, Lai A, et al: Altered functional connectivity of the default mode network in diffuse gliomas measured with pseudo-resting state fMRI. **J Neurooncol 116:**373–379, 2014
21. Hyvärinen A: Fast and robust fixed-point algorithms for independent component analysis. **IEEE Trans Neural Netw 10:**626–634, 1999
22. Ius T, Angelini E, Thiebaut de Schotten M, Mandonnet E, Duffau H: Evidence for potentials and limitations of brain plasticity using an atlas of functional resectability of WHO grade II gliomas: towards a "minimal common brain." **Neuroimage 56:**992–1000, 2011
23. Jenkinson M, Smith S: A global optimisation method for robust affine registration of brain images. **Med Image Anal 5:**143–156, 2001
24. Jenkinson M, Bannister P, Brady M, Smith S: Improved optimization for the robust and accurate linear registration and motion correction of brain images. **Neuroimage 17:**825–841, 2002
25. Kokkonen SM, Nikkinen J, Remes J, Kantola J, Starck T, Haapea M, et al: Preoperative localization of the sensorimotor area using independent component analysis of resting-state fMRI. **Magn Reson Imaging 27:**733–740, 2009
26. Kundu P, Brenowitz ND, Voon V, Worbe Y, Vértes PE, Inati SJ, et al: Integrated strategy for improving functional connectivity mapping using multiecho fMRI. **Proc Natl Acad Sci U S A 110:**16187–16192, 2013

27. Kundu P, Inati SJ, Evans JW, Luh WM, Bandettini PA: Differentiating BOLD and non-BOLD signals in fMRI time series using multi-echo EPI. **Neuroimage 60:**1759–1770, 2012
28. Liu H, Buckner RL, Talukdar T, Tanaka N, Madsen JR, Stufflebeam SM: Task-free presurgical mapping using functional magnetic resonance imaging intrinsic activity. **J Neurosurg 111:**746–754, 2009
29. Louis DN, Ohgaki H, Wiestler OD, Cavenee WK, Burger PC, Jouvet A, et al: The 2007 WHO classification of tumours of the central nervous system. **Acta Neuropathol 114:**97–109, 2007
30. Lutkenhoff ES, Rosenberg M, Chiang J, Zhang K, Pickard JD, Owen AM, et al: Optimized brain extraction for pathological brains (optiBET). **PLoS One 9:**e115551, 2014
31. Manglore S, Bharath RD, Panda R, George L, Thamodharan A, Gupta AK: Utility of resting fMRI and connectivity in patients with brain tumor. **Neurol India 61:**144–151, 2013
32. Margulies DS, Vincent JL, Kelly C, Lohmann G, Uddin LQ, Biswal BB, et al: Precuneus shares intrinsic functional architecture in humans and monkeys. **Proc Natl Acad Sci U S A 106:**20069–20074, 2009
33. McGirt MJ, Mukherjee D, Chaichana KL, Than KD, Weingart JD, Quinones-Hinojosa A: Association of surgically acquired motor and language deficits on overall survival after resection of glioblastoma multiforme. **Neurosurgery 65:**463–470, 2009
34. Mesulam M: Imaging connectivity in the human cerebral cortex: the next frontier? **Ann Neurol 57:**5–7, 2005
35. Mitchell TJ, Hacker CD, Breshears JD, Szrama NP, Sharma M, Bundy DT, et al: A novel data-driven approach to preoperative mapping of functional cortex using resting-state functional magnetic resonance imaging. **Neurosurgery 73:**969–983, 2013
36. Sair HI, Yahyavi-Firouz-Abadi N, Calhoun VD, Airan RD, Agarwal S, Intrapiromkul J, et al: Presurgical brain mapping of the language network in patients with brain tumors using resting-state fMRI: Comparison with task fMRI. **Hum Brain Mapp 37:**913–923, 2016
37. Quigley M, Cordes D, Wendt G, Turski P, Moritz C, Haughton V, et al: Effect of focal and nonfocal cerebral lesions on functional connectivity studied with MR imaging. **AJNR Am J Neuroradiol 22:**294–300, 2001
38. Raichle ME, Mintun MA: Brain work and brain imaging. **Annu Rev Neurosci 29:**449–476, 2006
39. Raichle ME: The restless brain. **Brain Connect 1:**3–12, 2011
40. Rosazza C, Aquino D, D'Incerti L, Cordella R, Andronache A, Zacà D, et al: Preoperative mapping of the sensorimotor cortex: comparative assessment of task-based and resting-state FMRI. **PLoS One 9:**e98860, 2014
41. Sanai N, Mirzadeh Z, Berger MS: Functional outcome after language mapping for glioma resection. **N Engl J Med 358:**18–27, 2008
42. Shimony JS, Zhang D, Johnston JM, Fox MD, Roy A, Leuthardt EC: Resting-state spontaneous fluctuations in brain activity: a new paradigm for presurgical planning using fMRI. **Acad Radiol 16:**578–583, 2009
43. Smith SM, Beckmann CF, Andersson J, Auerbach EJ, Bijsterbosch J, Douaud G, et al: Resting-state fMRI in the Human Connectome Project. **Neuroimage 80:**144–168, 2013
44. Smith SM, Fox PT, Miller KL, Glahn DC, Fox PM, Mackay CE, et al: Correspondence of the brain's functional architecture during activation and rest. **Proc Natl Acad Sci U S A 106:**13040–13045, 2009
45. Smith SM, Miller KL, Salimi-Khorshidi G, Webster M, Beckmann CF, Nichols TE, et al: Network modelling methods for FMRI. **Neuroimage 54:**875–891, 2011
46. Smith SM, Vidaurre D, Beckmann CF, Glasser MF, Jenkinson M, Miller KL, et al: Functional connectomics from resting-state fMRI. **Trends Cogn Sci 17:**666–682, 2013
47. Sporns O (ed): **Discovering the Human Connectome.** Cambridge, MA: MIT Press, 2012
48. Sporns O (ed): **Networks of the Brain.** Cambridge, MA: MIT Press, 2011
49. Stummer W, Meinel T, Ewelt C, Martus P, Jakobs O, Felsberg J, et al: Prospective cohort study of radiotherapy with concomitant and adjuvant temozolomide chemotherapy for glioblastoma patients with no or minimal residual enhancing tumor load after surgery. **J Neurooncol 108:**89–97, 2012
50. Stummer W, Pichlmeier U, Meinel T, Wiestler OD, Zanella F, Reulen HJ: Fluorescence-guided surgery with 5-aminolevulinic acid for resection of malignant glioma: a randomised controlled multicentre phase III trial. **Lancet Oncol 7:**392–401, 2006
51. van den Heuvel MP, Hulshoff Pol HE: Exploring the brain network: a review on resting-state fMRI functional connectivity. **Eur Neuropsychopharmacol 20:**519–534, 2010
52. van den Heuvel MP, Sporns O: Network hubs in the human brain. **Trends Cogn Sci 17:**683–696, 2013
53. van den Heuvel MP, Sporns O: Rich-club organization of the human connectome. **J Neurosci 31:**15775–15786, 2011
54. Wen PY, Macdonald DR, Reardon DA, Cloughesy TF, Sorensen AG, Galanis E, et al: Updated response assessment criteria for high-grade gliomas: response assessment in neuro-oncology working group. **J Clin Oncol 28:**1963–1972, 2010
55. Wink AM, Bullmore E, Barnes A, Bernard F, Suckling J: Monofractal and multifractal dynamics of low frequency endogenous brain oscillations in functional MRI. **Hum Brain Mapp 29:**791–801, 2008
56. Zhang D, Johnston JM, Fox MD, Leuthardt EC, Grubb RL, Chicoine MR, et al: Preoperative sensorimotor mapping in brain tumor patients using spontaneous fluctuations in neuronal activity imaged with functional magnetic resonance imaging: initial experience. **Neurosurgery 65 (6 Suppl):**226–236, 2009
57. Zhang D, Raichle ME: Disease and the brain's dark energy. **Nat Rev Neurol 6:**15–28, 2010

Disclosures

The authors report no conflict of interest concerning the materials or methods used in this study or the findings specified in this paper.

Author Contributions

Conception and design: Hart. Acquisition of data: Price. Analysis and interpretation of data: Hart, Suckling. Drafting the article: Hart. Critically revising the article: all authors. Reviewed submitted version of manuscript: all authors. Approved the final version of the manuscript on behalf of all authors: Hart. Statistical analysis: Hart, Suckling. Administrative/technical/material support: Price, Suckling. Study supervision: Suckling.

Supplemental Information

Previous Presentations

Portions of this work were presented in abstract form at the British Neurosurgery Research Group (BNRG) Meeting, Cardiff, United Kingdom, March 5–6, 2015.

Correspondence

Michael G. Hart, Division of Neurosurgery, Department of Clinical Neurosciences, Box 167, Cambridge Biomedical Campus, Cambridge CB2 0QQ, United Kingdom. email: mgh40@cam.ac.uk.